# AIAA-2000-4826
# Passive Load Alleviation in the Design of a Strut-Braced Wing Transonic Transport

F.H. Gern, A. Ko, E. Sulaeman, R.K. Kapania,
W.H. Mason, and B. Grossman
Virginia Polytechnic Institute and State University
Blacksburg, VA

and

R.T. Haftka
University of Florida
Gainesville, FL

8th AIAA/USAF/NASA/ISSMO
Symposium on
Multidisciplinary Analysis and Optimization
6-8 September 2000 / Long Beach, CA

# PASSIVE LOAD ALLEVIATION IN THE DESIGN OF A STRUT-BRACED WING TRANSONIC TRANSPORT AIRCRAFT

**Frank H. Gern[*], Andy Ko[†], Erwin Sulaeman[‡], Rakesh K. Kapania[§], William H. Mason[§], Bernard Grossman[¶]**
*Department of Aerospace and Ocean Engineering*
*Virginia Polytechnic Institute and State University*
*Blacksburg, VA 24061-0203*

**Raphael T. Haftka[**]**
*Department of Aerospace Engineering, Mechanical and Engineering Sciences*
*University of Florida*
*Gainesville, FL 32611-6250*

## Abstract

**This paper describes the multidisciplinary design optimization (MDO) of a transonic strut-braced wing aircraft. The optimization considers aeroelastic deformations of the wing and passive load alleviation. The calculations reveal that the strut twist moment provides substantial load alleviation and significant reductions in structural wing weight.**

**To benefit from the potential of appl ying passive load alleviation during preliminary aircraft design, a flexible wing sizing module has been linked to the MDO design tool to optimize the design of three different strut-braced wing aircraft configurations featuring fuselage mounted engines, underwing mounted engines, and wingtip mounted engines.**

## Introduction

Strut-braced wing configurations have been used both in the early days of aviation and today's small airplanes. In the beginning, adopting thin airfoil sections required external structural wing support to sustain the aerodynamic loads. However, external structures cause significant drag penalty. Gradually, it was understood that the external bracing could be removed and lower drag could be achieved by replacing the wing-bracing structure with a cantilever wing with an appropriate wing-box and thickness to chord ratios.

Along with the idea of the cantilever wing configuration with its aerodynamic advantages, the concept of the strut-braced wing configuration also survived. This is due to the tireless efforts of Werner Pfenninger from the early 1950s until the late 1980s[1]. Relative to a cantilever wing, a strut offers the opportunity to increase the wing aspect ratio and to decrease the induced drag significantly without wing weight penalties. Also, a lower wing thickness becomes feasible, reducing transonic wave drag and hence allowing lower wing sweep. Reduced wing sweep and high aspect ratio allow for natural laminar flow due to low Reynolds numbers and sweep. Consequently, a significant increase in the overall aircraft performance is achieved.[2,3]

A number of strut-braced wing aircraft configurations have been investigated in the past. In continuing Pfenninger's work, Kulfan and Vachal from Boeing performed preliminary design studies and evaluated the performance of a large subsonic military airplane.[4] They compared performance and economics of a cantilever wing with a strut-braced

[*] Research Associate, now: Research Assistant Professor, Center for Intelligent Material Systems and Structures, Member AIAA
[†] Graduate Student, Student Member AIAA
[‡] Graduate Student
[§] Professor, Associate Fellow AIAA
[¶] Department Head and Professor, Associate Fellow AIAA
[**] Distinguished Professor, Fellow AIAA

wing configuration. Two load conditions, a 2.5g maneuver and 1.67g taxi bump were used to perform structural analyses.

The strut resolved a ground strike problem during taxiing encountered by the cantilever design. Moreover, the strut-braced wing configuration required less fuel (1.6%), and resulted in lower takeoff gross weight (1.8%) and lower empty weight (3%) compared to the cantilever wing configuration. Cost comparisons showed that the operating costs of the strut-braced wing configuration were slightly less than those of the cantilever wing configuration because of its lower takeoff gross weight.

Park[5] compared the block fuel consumption of a strut-braced wing versus a cantilever wing. Even though he concluded that the use of a strut saves structural wing weight, the significant increase in the strut thickness to cope with its buckling at the -1.0g load condition increased the strut drag. Therefore, a strut did not appear practical for this transport aircraft due to an increased fuel consumption compared to the cantilever design.

The strut-buckling problem was addressed in our previous work[3,7,8] through an innovative concept of a telescoping sleeve mechanism that activates the strut only during positive g maneuvers. For negative g maneuvers, the wing acts like a cantilever wing. Furthermore, this arrangement allows a defined strut force at the 2.5g maneuver design load instead of the statically indeterminate one obtained from a rigid strut attachment. This defined strut force as well as strut position can be optimized in order to achieve the maximum benefits from the design concept.

Another study on strut-braced wing configurations was conducted by Turriziani et al.[6] They addressed fuel efficiency advantages of a strut-braced wing business jet employing an aspect ratio of 25 over an equivalent conventional wing business jet with the same payload range. They concluded that the strut-braced wing configuration reduces the total aircraft weight, even though wing and strut weight increased compared to the cantilever wing case, which is due to aerodynamic advantages of high aspect ratio wings. Furthermore, the results showed a fuel weight savings of 20%.

The reduced wing thickness together with shorter wing chords associated with strut-braced wings significantly reduce wing-box torsional stiffness and render the wing more sensitive to aeroelastic problems like increased static aeroelastic deformation or reduced flutter and divergence speeds. The present work highlights a possibility of resolving the problem of increased aeroelastic deformations by employment of the strut moment induced on the wing.

To fully exploit the synergism from the strut-braced wing concept, an MDO approach has been chosen for aircraft design optimization. The multidisciplinary team consists of aerodynamics, structures, and a detailed investigation of interference drag. The aerodynamic analysis uses simple models for induced drag, parasite drag, and interference drag. All analyses are linked together, and the performance of the strut-braced wing aircraft is then optimized for minimum take-off gross weight.[3,7,8]

The MDO approach has been implemented in several aircraft designs. Grossman et al.[9] investigated the interaction of aerodynamic and structural design of a composite sailplane subject to aeroelastic, structural, and aerodynamic constraints to increase the overall performance. They showed that the multidisciplinary design can yield results superior to the ones obtained from the sequential method. Another example is the application of MDO to a High Speed Civil Transport (HSCT). A significant effort has been made at the Multidisciplinary Analysis and Design (MAD) Center of Virginia Tech to perform MDO of an HSCT. Several methods were developed for the better use of the MDO approach for aircraft conceptual and preliminary design. More information about this work can be obtained from Refs. 10 and 11.

A wing sizing module developed within this project provides two essential features within the MDO environment. First, it is used to calculate the structural wing weight, i.e. the bending material weight of the wing-box. It has been found that commonly available wing weight calculation routines like the NASA Langley developed Flight Optimization System (FLOPS)[12] are not accurate enough in accounting for the effect of the strut. Therefore, a program has been developed to accurately calculate the bending material weight of the wing based on a hexagonal wing-box model. The non-structural wing weight like flaps, slats, spoilers, ribs etc. is still calculated from the FLOPS equations by replacing the FLOPS bending material weight by the actual one.

Cantilever baseline design configuration

Fuselage mounted engine strut-braced wing design

Wing mounted engine strut-braced wing design

Tip mounted engine strut-braced wing design

**Figure 1:** General configuration layouts of different investigated designs

The benefits of a strut-braced wing configuration also result in a drag penalty due to the strut. In particular, the potential interference drag penalty at the junction of the strut with the fuselage and the wing is more difficult to estimate than the drag of the main body of the strut. In the vicinity of the junctions, detrimental effects such as unwanted shock waves and flow separation can cause the interference drag to increase significantly. Therefore, an Euler analysis was used for assessing interference drag. Since it is not computationally feasible to include the Euler solution inside the optimization, a response surface is created to approximate the dependence of the interference drag on the strut angle and strut thickness to chord ratio. A vertical strut offset was used as to achieve a significant reduction in wing/strut interference drag.

## Optimization Methodology

Four different aircraft configurations were being considered: Cantilevered Wing, Fuselage Mounted Engines SBW, Wing Mounted Engines SBW and Tip Mounted Engines SBW. The cantilever design is being used as a baseline comparison, to which we can compare weight savings and differences in design. It also serves as a validation case with which we can compare with existing aircraft. The general configuration of the designs is shown in **Figure 1**. The primary mission profile will require a 325 passenger load, Mach 0.85 cruise speed, and a 7500 nautical mile range with an additional 500 nautical miles as reserve (**Figure 2**).

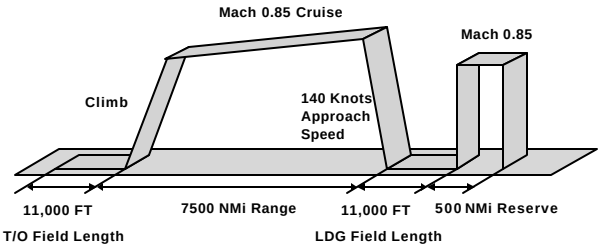


**Figure 2:** Mission profile

**Table 1:** Optimization constraints

| Description | Constraint |
|---|---|
| Range | Calculated range > 7500nm |
| Initial cruise rate of climb | Initial cruise ROC > 500 ft/min |
| Max. allowable cruise section $C_l$ | Calculated maximum cruise section $C_l$ < 0.8 |
| Fuel capacity | Fuel weight < Fuel capacity |
| Engine-out | Required $C_n$ < Available $C_n$ |
| Wing deflection | Wing deflection < 20 ft. |
| Second segment climb gradient | Calculated gradient > 0.024 |
| Balanced field length | Balanced field length < 11000 ft. |
| Approach velocity | Approach velocity < 140 knots |
| Missed approach climb gradient | Calculated gradient > 0.021 |
| Landing distance | Landing distance < 11000 ft. |
| Slack load factor upper limit | Strut slack load factor < 0.8 |
| Slack load factor lower limit | Strut slack load factor > 0.0 |

For optimization, the Virginia Tech Strut-Braced Wing code uses the method of feasible directions implemented in the Design Optimization Tools (DOT) software developed by Vanderplatts R&D.[17] The objective is to minimize the Take-Off Gross Weight (TOGW) of the aircraft. This is the traditional objective of large transport designs and is a good measure of the total system cost.[25]

To maximize the beneficial influence of the strut upon the wing structure, strut force and spanwise position of the wing-strut intersection are optimized by the MDO code for the 2.5g maneuver load case. To attain acceptable aerodynamic characteristics of the strut an airfoil cross section is considered. The strut is designed in a way that it will not carry an aerodynamic load during the cruise condition.

Depending on the configuration considered, a total of 15 to 22 design variables were used. These include wing half-span, chords, thickness to chord ratios, strut position and geometry, engine location, thrust, and cruise altitude. Each design variable is given upper and lower side constraints and then scaled to take a value between 0 and 1.

A total of 13 inequality constraints were enforced in the optimization These constraints reflect typical restrictions on passenger transport aircraft. **Table 1** lists these constraints.

## Structural Wing Modeling

Due to the unconventional nature of the proposed wing concept, commonly available weight calculation models for transport aircraft (such as the NASA Langley developed Flight Optimization System FLOPS[12]) are not accurate enough. A special bending weight calculation procedure was thus developed.

### Load Cases

To determine the bending material weight of the strut-braced wing, two maneuver load conditions (2.5g maneuver, -1.0g pushover) and a taxi bump (-2.0g) are considered to be design critical. For the -1.0g pushover and for the -2.0g taxi bump, the strut is not active and the wing acts like a cantilever beam. Since the strut is not supporting the wing in these cases, high deflections of the wing occur for the -2.0g taxi bump. As a result, an optimization procedure is implemented to distribute the bending material to prevent wing ground strikes.

### Strut Slack Load

The optimization of the strut force discussed before means that the strut first engages in tension at some positive load factor. This can be achieved by providing a mechanism that unloads the strut tension below a certain load factor. The optimum strut force at 2.5g is then different from the strut force that would be obtained at 2.5g if the strut was engaged for all positive values of the load factor.

The slack load factor is defined as the load factor at which the strut initially engages. It is important to have the slack load factor always positive, otherwise the strut would be pre-loaded at the jig shape of the wing to achieve the optimum strut force. To prevent the strut from repeatedly engaging and disengaging

during cruise due to gust loads, the upper limit for the slack load factor is set to 0.8 during the optimization.

### Wing-Box Model

A hexagonal wing-box model was implemented into the wing weight calculation module for structural wing sizing (**Figure 3**). This model was provided by Lockheed Martin Aeronautical Systems in Marietta, Georgia. Based upon Lockheed Martin's experience in wing sizing, the wing-box geometry varies in the spanwise direction with optimized area and thickness ratios for spar webs, spar caps, stringers, and skins. By keeping these ratios fixed, it is still possible to reduce all geometric data of the wing-box to one independent thickness, which is allowed to vary in the spanwise direction. Therefore, despite the complexity of the geometry, a closed-form solution for the material thickness can still be found by employing a piecewise linear load representation.

The hexagonal wing-box allows computation of bending and torsional stiffness with a high degree of accuracy. This torsional stiffness becomes essential when calculating wing twist and flexible wing spanload, as well as for the incorporation of aeroelastic constraints into design optimization. Furthermore, minimum gauges and maximum stress cutoffs can be accurately applied.

## Aerodynamics for Wing Sizing

The aerodynamic loads are calculated based on the vortex lattice method (VLM). For this purpose, a linearized transonic VLM code was developed. To account for compressibility effects, the airflow density is corrected according to the freestream Mach number

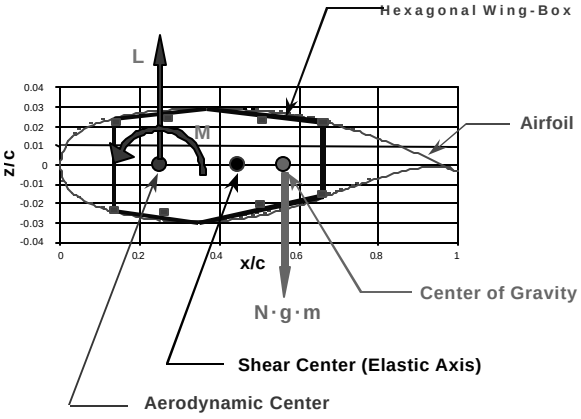


**Figure 3:** Hexagonal wing-box and applied sectional forces and moments

using the internal Prandtl-Glauert correction. Although not capable of transonic shock predictions, this modification allows an acceptable prediction of local lift coefficients. To take into account the spanwise variation of the sectional pitch and dihedral, as well as the chordwise variation of the airfoil camber surface, the flow tangency boundary condition is formulated as:

$$U_\infty \sin(\alpha - \delta)\cos\gamma = w_{ab}\cos\gamma\cos\delta + v_{ab}\sin\gamma\cos\delta - u_{ab}\cos\gamma\sin\delta$$

where $\alpha$, $\delta$ and $\gamma$ are the angle of attack, slope of the mean camber line, and dihedral, respectively, for each point on the curved surface. The induced velocities $u_{ab}$, $v_{ab}$ and $w_{ab}$ represent the backwash, sidewash and downwash velocities, respectively, acting on any arbitrary point C $(x_c,y_c,z_c)$ of the lifting surface due to a bound vortex AB having the vortex strength $\Gamma$ and the end points A $(x_a,y_a,z_a)$ and B $(x_b,y_b,z_b)$. A detailed description of the aerodynamic load calculation can be found in Ref. 15.

## Passive Load Alleviation

### Wing Sizing Process

For accurate wing sizing, the wing was subdivided into 81 structural nodes representing the spanwise grid points for the application of the piecewise linear loads. To account for increasing gradients in the spanload towards the wing tip, cosine spacing was used. The aerodynamic lifting surface features 40 spanwise and 5 chordwise vortex panels distributed equally along the wing span. To reduce computational time, the number of chordwise vortex panels can be reduced to one, thus reducing the lifting surface theory to lifting line aerodynamics. In order to assure reliable optimization results, a comprehensive assessment of the influence of the vortex paneling upon wing weight has been conducted.

**Figure 4** depicts the influence of the number of chordwise vortex panels on the calculated wing weight for a 747 type wing. Reduction of the number of chordwise panels proved to significantly reduce runtime. However, this runtime reduction comes along with an increased wing weight, therefore leading to more conservative optimization results. The pre-twist of the wing planform is calculated using Lamar's design program LAMDES.[13] Due to this pre-twist calculation, the LAMDES module showed a much higher sensitivity to panel reductions.

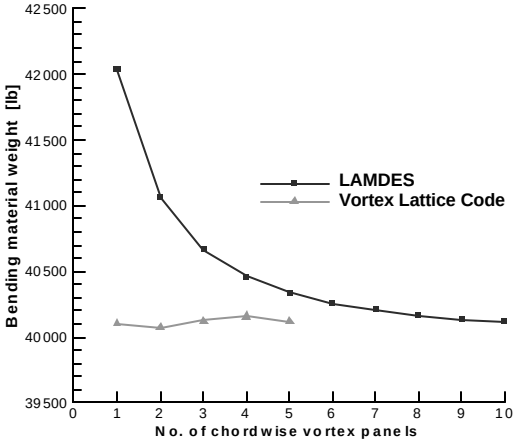


**Figure 4:** Calculated wing bending material weight vs. number of chordwise vortex panel for both aerodynamic modules

Therefore, the lower limit for the number of chordwise panels in LAMDES was set to six, representing a reasonable compromise between reduced runtime and reliable wing sizing.

The initial wing deformation including sectional twist angle, dihedral (bending slope) and deflection, is calculated from the rigid wing spanload. which usually is close to an elliptical one. To obtain an elliptical lift distribution during cruise, the wing is being pre-twisted and jig twisted. Since, for a swept wing, the sectional streamwise angle of attack is a combination of twist angle and bending slope, the wing bending deformation significantly influences the aerodynamic effectiveness of the lifting surface. Therefore, to achieve the desired twist distribution of the wing during cruise, the wing is jig twisted to account for the changes in the local twist due to the bending deformation.

Gimmestad from Boeing showed that consideration of the jig twist for wing sizing of the B-52 resulted in a 10% reduction in the design loads.[14] Therefore, considering the jig twist during preliminary design may result in significant structural weight savings.

The lift distribution is recalculated iteratively based on the actual wing deformation, yielding a new (flexible) spanload. From there, all structural wing parameters like bending stiffness, torsional stiffness, and wing weight are recalculated and then again used for computation of the flexible spanload. A detailed description of the wing sizing process is given in Ref. 15.

The total wing weight, including the secondary structure like ribs, flaps etc. is calculated using the FLOPS equations.[12] For this purpose, only the bending material weight in FLOPS is replaced by the bending material weight obtained from the present model.

### Validation

The structural design code was validated using available data for the 747-100. The bending material weight computed from the piecewise linear load model was compared with the bending material weights given by Torenbeek[16] and FLOPS.[12] Comparison of the results obtained using the present structural model with the actual 747-100 weights for both the assumption of an elliptical spanload as well as for the consideration of passive load alleviation showed good agreement.[15]

## Strut-Braced Wing Sizing

### Flexible Wing Spanload

The strut-braced wing has been analyzed and sized using the new module. As an example, the wing sizing process is described for the underwing mounted engine configuration. **Figure 5** shows the spanload distribution on the wing for the 2.5g maneuver obtained from the iterative process.

In **Figure 5**, spanload and structural wing weight are converged to their final values. For the strut attached at the elastic axis of the wing, the strut-braced wing exhibits the same load alleviation

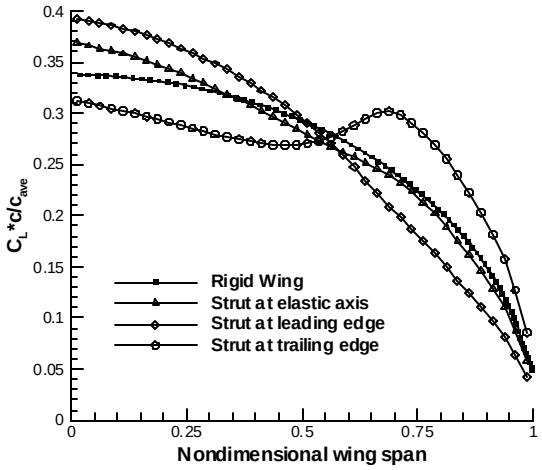


**Figure 5:** Spanload distribution for the wing mounted engine strut-braced wing in a 2.5g maneuver

behavior as its cantilever counterpart. Due to the upward bending of the wing, lift loads are shifted inboard because of the reduction of the sectional angle of attack on the outboard wing sections (wash-out). For a rigid wing, the spanload for the 2.5g maneuver would be approximately the cruise spanload scaled by the load factor 2.5, i.e. an almost elliptical one. Compared to a conventional cantilever wing, the wash-out effect for the strut-braced wing is relatively weak.

The two main reasons for this behavior are:

a) The torsional stiffness of the wing box is low. This allows the wing sections to rotate more, thus compensating in part for the angle of attack reduction due to the upward bending of the wing.

b) The strut significantly reduces the upward bending of the wing. This bending deflection is the main component adding to the wash-out effect of swept back wings.

**Figure 5** also depicts one major advantage of the strut-braced wing from the aeroelastic point of view: a chordwise offset of the strut attachment to the wing-box produces a twist moment acting on the wing. By attaching the strut to the leading edge instead of the wing elastic axis, this moment literally twists down the wing leading edge. As a result, even more load is shifted inboard, producing a much higher load alleviation effect than for a conventional wing.

To further highlight the strut influence upon the load alleviation behavior and wing spanload, the influence of a strut attached to the trailing edge is also illustrated in **Figure 5**. In this case, the strut moment twists the leading edge of the wing upward, thus increasing the aerodynamic loads on the outboard wing sections. To sustain the total lift for the respective load factor also when considering wing flexibility, the aircraft incidence has been adjusted after each iteration step.[8]

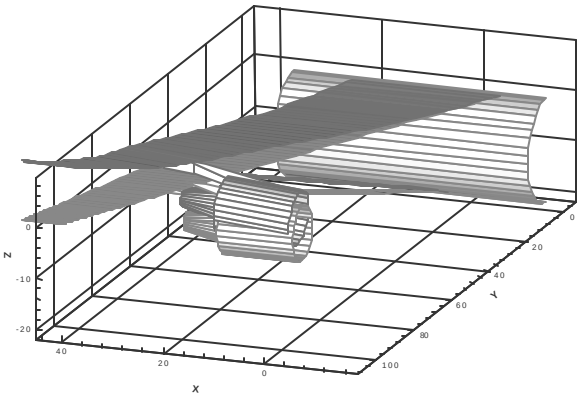


**Figure 6:** 2.5g maneuver deformation for the wing mounted strut-braced wing configuration.

**Wing Sizing From Flexible Spanload**

Consideration of the actual maneuver spanloads usually results in a significant reduction in the design loads.[14] Since the influence of the strut moment offers even more potential for maneuver load alleviation, the impact of flexible wing sizing may even be higher than for the cantilever wing. Therefore, the wing structure has been resized according to the actual spanload distribution after each iteration step.

Weight calculation from the flexible design loads reveals the significant influence of the strut moment on maneuver load alleviation and wing weight. The influence of the chordwise strut offset on the calculated wing bending material weight for several different chordwise strut positions, varying from the leading edge to the trailing edge, has also been shown in Ref. 15. In addition, the center of gravity of the engine can been moved in the chordwise direction as well. This way, two additional twist moments influence the aeroelastic deformations, spanload, and wing weight. Compared to the rigid wing weight, sizing the wing using the actual design loads and considering the appropriate chordwise positions of engine and strut can be used to lower structural weights for most configurations.

It is important to note that an identical wing featuring a thin airfoil would suffer a significant weight penalty if designed without a strut. Calculations for a fuselage mounted engine configuration indicate a 43% weight penalty for the rigid wing sizing and a 29% weight penalty for the flexible design loads in such a case.[15] The impact of the strut and engine position of the wing's deformation behavior is highlighted in **Figure 6**. For the configuration yielding the lowest wing weight, maneuver deformations are relatively small. Even more, the wing twist is significantly reduced. In contrast, placing the strut at the trailing edge would result in higher aeroelastic loads, maneuver deformations, and wing weight (not depicted).

## Aerodynamic Modeling

The aerodynamics model consists of a combination of response surface equations developed from CFD analysis and theoretical models. The drag components that are modeled are parasitic, induced,

wave and interference drag. A detailed discussion of these drag models can be found in previous Virginia Tech SBW studies.[7,21]

The parasitic drag model is based on applying form factors to an equivalent flat plate skin friction drag analysis. The amount of laminar flow on the wing and tails is estimated by interpolating results from the Reynolds number vs. sweep data obtained from the F-14 Variable Sweep Transition Flight Experiment (1984-1987) and the Boeing 757 Natural Laminar Flow Glove Flight Test (1985).[22] For the fuselage, nacelles and pylon friction drag, an input Reynolds number is used to determine the transition location on those components. The form factors that are then applied are calculated using formulas supplied by Lockheed Martin Aeronautical Systems.

To calculate induced drag, a discrete vortex method in the Trefftz plane is being used.[26] This gives the optimum load distribution corresponding to the minimum induced drag for an arbitrary, non-coplanar wing/strut configuration.

The interference drag of the wing, strut, and fuselage intersections are estimated using Hoerner equations based on subsonic wind tunnel tests.[18] To alleviate the problem associated with a sharp wing-strut angle, the strut employed here is given the shape of an arch and intersects the wing perpendicularly. Analyses for an arch radius varying from 1 ft to 4 ft were performed with CFD tools. Unstructured grids were obtained with the advancing-front methodology implemented in the code VGRIDns. The Euler equations were then solved using the CFD code USM3D at the cruise Mach number of 0.85.[19,20]

## Weights Formulation

To calculate the individual component weights of the aircraft, equations from NASA Langley's Flight Optimization System (FLOPS)[12] and proprietary equations supplied by Lockheed Martin Aeronautical Systems (LMAS) were used. The wing bending material weight is obtained from the aforementioned wing sizing module. In addition to this, technology factors are applied to the different weight groups to simulate technology advances expected by the year 2010. The factors were compiled and supplied by LMAS after a detailed study to assess technology advances in different areas. These advances include effects of riblets on the fuselage and nacelles, supercritical airfoils, induced drag reduction, integrated flight control systems, fly by light and power by light, simple high lift devices, and composite wing and tail. A detailed discussion of the material used in the weights models can be found in Ref. 21.

## Stability and Control

FAR specifications require that an aircraft must be able to maintain straight flight at 1.2 times the stalling speed with one engine inoperative. It allows a maximum bank angle of 5º with some sideslip angle. The vertical tail is sized using a tail volume coefficient method to meet these FAR requirements through an inequality constraint. The lateral force provided by the vertical tail provides most of the required yawing moment needed to maintain straight flight in an engine-out condition. However, for the tip mounted engine configuration, circulation control is used on the vertical tail to augment the force provided by the vertical tail. The vertical tail lift coefficient due to circulation control is limited to an upper bound of 1.0. To calculate the stability derivatives, a modified DATCOM empirical method was used. Ref. 27 provides a more detailed explanation of the stability and control model.

## Propulsion

GE-90 class, high-bypass ratio turbofan engines are used in this study. The engine deck for a GE-90 like engine was obtained from LMAS, and the necessary variables such as specific fuel consumption and maximum thrust at cruise altitude are being obtained through interpolation from a least square fit to the data. A rubber engine sizing method was used to scale the GE-90 class engine to meet thrust requirements.

## Performance

The range is calculated using the Breguet range equation. To take into account the fuel burned during the climb segment to initial cruise altitude, 95.6% of the TOGW is used as the initial weight in the range calculation. The lift to drag ratio, flight velocity and specific fuel consumption are taken for an average cruising altitude and Mach number. An additional 500 nautical mile range requirement is added to the range of the aircraft to account for the reserve fuel weight.

To calculate field performance constraints, methods found in Roskam and Lan[23] are used. The field performance parameters that are considered are

the second segment climb gradient, balanced field length, missed approach climb gradient and landing distance. These parameters are calculated for hot day conditions at sea level. The second segment climb gradient is calculated as the ratio of the rate of climb to the forward velocity at full throttle with one engine inoperative was used. The balanced field length was calculated based on the empirical estimation from Torenbeek.[24] The missed approach climb gradient is similar to the second segment climb gradient, but with only 73% of the TOGW, and with all engines operating. The landing distance is defined as the distance from a 50-ft obstacle (clearance to the touchdown including flare distance) to the aircraft full stop. See Ref. 21 for a more detailed discussion of the field performance estimation.

## Optimization Results

### Validation

To validate the MDO code, each component was individually tested with data from existing transport aircraft. In addition, the optimization results were reviewed by LMAS, who compared it with their own studies. The overall MDO code was validated by comparison with the Boeing 777-200IGW configuration. In this case, a cantilever wing design with all technology factors set to a value of one (i.e. representing 1995 technology levels) was optimized. The MDO code showed good agreement with respect to both the TOGW and wing weight. The cantilever wing design produced a TOGW of 592,000 lbs. while the TOGW of the Boeing 777-200IGW was listed in Jane's as 590,000 lbs. Also, the geometric properties of the cantilever wing design were similar to that of the Boeing 777-200IGW.

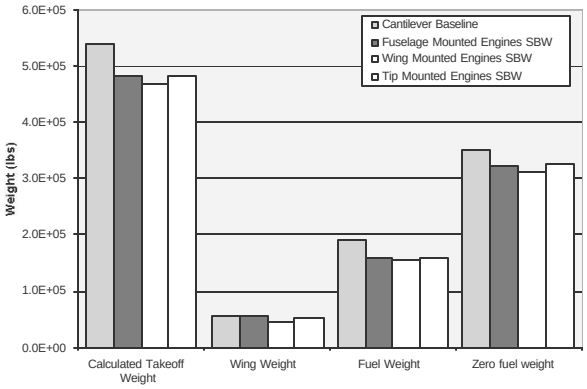


**Figure 7:** Comparison of weight components with passive load alleviation

### Comparison with cantilever wing baseline

Two different comparisons are made with regard to the use of the structures model in the overall optimization of the strut-braced wing aircraft:

a) The first compares the different SBW designs with the baseline cantilever wing design. This comparison is made with optimum designs obtained using the flexible wing structures model.

b) The influence of passive load alleviation is demonstrated by comparing similar optimized SBW designs with rigid and flexible wing sizing applied. Here we highlight the advantages and disadvantages in implementing such a model in the design optimization of the SBW aircraft.

**Figure 7** and **Table 2** compare the component weights for the four aircraft configurations analyzed. For comparison purposes, **Table 3** shows the optimization results from rigid wing sizing. It can be seen that the SBW design has a TOGW weight savings of up to almost 14% compared to the baseline cantilever design. The wing-mounted engine SBW design gave the best savings in TOGW. Most of the differences can be seen in the fuel weight, with as much as 19% in the case of the wing mounted engines SBW design. Coupled with a reduction of more than 20% in required engine thrust, the SBW design would also have less exhaust and noise emissions compared to a cantilever design. In general, the SBW designs have lower wing sweep angles and smaller thickness to chord ratios, which would result in better laminar flow over the wings. Also, the SBW designs have lower thrust to weight ratios and wing loading.

Although the Fuselage Mounted Engines SBW and Wing Mounted Engines SBW have higher wing spans compared to the cantilever baseline configuration, it is within the current 80m airport gate spacing. The Tip-Mounted Engines SBW design has a shorter wing span due to the Engine-Out Constraint which is active for this case. Due to the huge moments created during an engine-out condition, the optimizer found that decreasing the wing span would meet the constraint without an excessive weight penalty. We also notice that the Second Segment Climb Gradient constraint is active for all the design cases. This constraint usually drives the required thrust of the aircraft and is an important constraint that needs to be considered in the design of the SBW aircraft.

**Table 2:** Optimization results from flexible wing sizing

| | Cantilever | Fuselage Mounted Engines SBW | Wing Mounted Engines SBW | Tip Mounted Engines SBW |
|---|---|---|---|---|
| Wing Half-Span (ft) | 104.97 | 110.39 | 107.97 | 103.99 |
| Wing 1/4-Chord Sweep (deg) | 37.93 | 31.43 | 32.56 | 30.99 |
| Strut 1/4-Chord Sweep (deg) | | 22.67 | 20.49 | 30.93 |
| Wing Average Chord (ft) | 15.83 | 16.98 | 17.02 | 17.94 |
| Strut Chord (ft) | | 6.70 | 7.10 | 4.70 |
| Wing Average t/c | 0.1142 | 0.0910 | 0.0951 | 0.1048 |
| Engine Thrust (lbs) | 73232.8 | 58949.9 | 57749.9 | 63890.8 |
| Thrust to Weight Ratio | 0.2710 | 0.2450 | 0.2475 | 0.2640 |
| Wing Loading (lb/ft^2) | 121.76 | 117.68 | 118.81 | 113.19 |
| **Takeoff Gross Weight (lbs)** | **540540.9** | **481319.0 (-11.0%)** | **466697.2 (-13.7%)** | **484070.2 (-10.4%)** |
| **Wing Weight (lbs)** | **55799.6** | **54469.8 (-2.38%)** | **45998.6 (-17.6%)** | **53079.4 (-4.87%)** |
| **Fuel Weight (lbs)** | **190703.8** | **157282.6 (-17.5%)** | **154768.4 (-18.8%)** | **158672.0 (-16.8%)** |
| **Zero fuel weight (lbs)** | **349837.2** | **324036.4 (-7.38%)** | **311928.8 (-10.8%)** | **325398.1 (-6.99%)** |
| **Active Constraints** | | | | |
| Section Cl Constraint | ACTIVE | ACTIVE | ACTIVE | ACTIVE |
| Engine-Out Constraint | | | | ACTIVE |
| Wingtip Deflection Constraint | | | | |
| Second Segment Climb Constrair | ACTIVE | ACTIVE | ACTIVE | ACTIVE |
| Balanced Field Length Constraint | | ACTIVE | ACTIVE | |

**Table 3**: Optimization results from rigid wing sizing.

| | Cantilever | Fuselage Mounted Engines SBW | Wing Mounted Engines SBW | Tip Mounted Engines SBW |
|---|---|---|---|---|
| Wing Half-Span (ft) | 104.02 | 110.45 | 107.80 | 103.09 |
| Inboard Wing 1/4-Chord Sweep (deg) | 36.57 | 31.02 | 28.54 | 30.83 |
| Strut 1/4-Chord Sweep (deg) | | 22.97 | 21.58 | 31.06 |
| Wing Average Chord (ft) | 16.41 | 17.08 | 17.03 | 17.89 |
| Strut Chord (ft) | | 6.69 | 7.21 | 4.76 |
| Wing Average t/c | 0.1132 | 0.0909 | 0.0967 | 0.1052 |
| Engine Thrust (lbs) | 76365.6 | 60213.5 | 60144.1 | 63586.7 |
| Thrust to Weight Ratio | 0.2758 | 0.2460 | 0.2530 | 0.2652 |
| Wing Loading (lb/ft^2) | 122.48 | 118.16 | 121.78 | 113.45 |
| **Takeoff Gross Weight (lbs)** | **553852.1** | **489488.9 (-11.6%)** | **475442.8 (-14.2%)** | **479561.1 (-13.4%)** |
| **Wing Weight (lbs)** | **59993.4** | **58019.9 (-3.29%)** | **46806.0 (-22.0%)** | **49946.6 (-16.7%)** |
| **Fuel Weight (lbs)** | **196744.9** | **160570.1 (-18.4%)** | **160970.1 (-18.2%)** | **157895.4 (-19.7%)** |
| **Zero fuel weight (lbs)** | **357107.2** | **328918.9 (-7.89%)** | **314472.7 (-11.9%)** | **321665.7 (-9.92%)** |
| **Active Constraints** | | | | |
| Section Cl Constraint | ACTIVE | ACTIVE | ACTIVE | ACTIVE |
| Engine-Out Constraint | | | | ACTIVE |
| Wingtip Deflection Constraint | | | ACTIVE | ACTIVE |
| Second Segment Climb Constraint | ACTIVE | ACTIVE | | ACTIVE |
| Balanced Field Length Constraint | | ACTIVE | ACTIVE | |

## Influence of passive load alleviation

**Figure 8** compares the TOGW of the investigated configurations with and without flexible wing sizing. There is little difference in the geometric properties of the designs obtained for rigid and flexible wing structural sizing. For the two different wing sizing models, the TOGW savings over a similarly designed cantilever wing aircraft have been compared. **Tables 2 and 3** show that the impact of flexible wing sizing on the weight savings of the SBW over the cantilever design is relatively small. Weight savings obtained for the SBW designs using flexible wing sizing are in the same order of magnitude like the weight gains obtained using rigid wing sizing. As a result, flexible wing sizing has little effect on the overall weight optimization results. However, flexible wing sizing allows savings of 3000-4000 lbs in wing weight, which are augmented by reduced fuel weight and reduced engine thrust, leading to about 8000-13000 lbs savings in TOGW.

The cantilever wing benefits more from the flexible load calculation than the SBW wings. First, the change in wing weight is slightly larger. Also, the cantilever wing is able to reduce the wing chord and increase the wing span, thereby increasing the aspect ratio, reducing the drag and having a much larger gain in fuel consumption.

An exception to these trends is the Tip Mounted Engines SBW design where an increase in wing weight is observed. The cause for this reversal in trend is an increase in wing loading on the outboard wing sections due to the inertia of the tip mounted engine during maneuvers.

It is also noticed that for the Wing Mounted Engines SBW and Tip Mounted Engines SBW design, the wing deflection constraint is active when designed using the rigid wing model while it is inactive using the flexible wing model. In the case of the Wing Mounted Engines SBW design, the difference in the wing deflection between both cases is 1.2 ft. However, for the Tip Mounted Engines design, this difference is in the order of four feet.

Another difference in the use of the flexible wing sizing model is in optimization run time. With the rigid wing sizing model, it takes approximately 2 seconds per aerodynamic analysis and the corresponding structural design. This corresponds to approximately 15-20 minutes for the MDO optimization. However, with flexible wing sizing, it takes approximately 17 seconds per analysis and structural design, and 2-3 hours for the MDO optimization. Hence, to reduce runtime, an


**Figure 8:** Comparison of TOGW between rigid and flexible wing sizing.

optimization is conducted using the rigid wing sizing model first. Then, the optimization is restarted using flexible wing sizing, with the previous optimum design as the starting point. This reduces the MDO optimization run time to less than an hour.

## Conclusions

A Multidisciplinary Design Optimization procedure of a strut-braced wing transonic transport aircraft has been developed. Wing structural weight is obtained using flexible wing spanloads and a specially developed wing sizing module. Validation of the module with an existing aircraft wing and comparison with results from other sources showed very good agreement.

The calculations revealed the significant influence of the strut on the bending material weight of the wing. The use of a strut enables one to design a wing with thin airfoils without a weight penalty. Designing an identical thin airfoil wing without a strut would result in a 40% increase in wing weight.

The strut position affects spanload distributions and wing deformations. Weight savings are possible by calculation and iterative resizing of the wing structure according to the actual design loads. Moreover, as an advantage over the cantilever wing, employment of the strut twist moment for further load alleviation leads to increased savings in structural weight. As a result, the strut moment can be used to recover some of the gains lost due to the strut restriction of the wing bending.

## Acknowledgments

This project was funded by NASA Langley Grant NAG-1-2217 with Dr. Mark Moore as a grant monitor. Part of the work was done under subcontract from Lockheed Martin Aeronautical Systems in Marietta, Georgia. The authors would like to thank Bob Olliffe from Lockheed Martin Aeronautical Systems for the valuable input and discussions concerning the structural data for the hexagonal wing-box model. They also would like to thank their team members Joe Schetz and Philippe-André Tétrault for their contributions regarding the wing/strut interference drag calculation.

## References

[1]Pfenninger, W., "Design Considerations of Large Subsonic Long Range Transport Airplanes with Low Drag Boundary Layer Suction," Northrop Aircraft, Inc., Report NAI-58-529 (BLC-111), 1958. (Available from DTIC as AD 821759)

[2]Joslin, R.D., "Aircraft Laminar Flow Control," *Annual Review of Fluid Mechanics*, Annual Reviews Inc., Vol. 30, pp. 1-29, Palo Alto, CA, 1998.

[3]Grasmeyer, J.M., Naghshineh-Pour, A.H., Tetrault, P.A., Grossman, B., Haftka, R.T., Kapania, R.K., Mason, and W.H., Schetz, "Multidisciplinary Design Optimization of a Strut-Braced Wing Aircraft with Tip-Mounted Engines," MAD Center Report 98-01-01, Virginia Tech, January 1998.

[4]Kulfan, R.M., and Vachal, J.D., "Wing Planform Geometry Effects on Large Subsonic Military Transport Airplanes," Boeing Commercial Airplane Company, AFFDL-TR-78-16, February 1978.

[5]Park, H. P., "The Effect on Block Fuel Consumption of a Strutted vs. Cantilever Wing for a Short Haul Transport Including Strut Aeroelastic Considerations," AIAA Paper 78-1454, Aircraft Systems and Technology Conference, Los Angeles, CA, 7 p., Aug. 21-23, 1978.

[6]Turriziani, R.V., Lovell, W.A., Martin, G.L., Price, J.E., Swanson, E.E., and Washburn, G.F., "Preliminary Design Characteristics of a Subsonic Business Jet Concept Employing an Aspect Ratio 25 Strut Braced Wing," NASA CR-159361, October 1980.

[7]Grasmeyer, J.M., "Multidisciplinary Design Optimization of a Strut-Braced Wing Aircraft," MS Thesis, Virginia Tech, April 1998.

[8]Gern, F.H., Gundlach, J.F., Ko, A., Naghshineh-Pour, A., Sulaeman, E., Tetrault, P.-A., Grossman, B., Kapania, R.K., Mason, W.H., J.A. Schetz, and Haftka, R.T., "Multidisciplinary Design Optimization of a Transonic Commercial Transport with a Strut-Braced Wing," SAE Paper 1999-01-5621, 1999 World Aviation Congress, San Francisco, CA, Oct. 19-21, 1999,

[9]Grossman, B., Strauch, G.J., Eppard, W.M., Gurdal, Z., and Haftka, R.T., "Integrated Aerodynamic/Structural Design of a Sailplane Wing," AIAA-86-2623, Dayton, Ohio, October 20-22, 1986.

[10]Giunta, A.A., Balabanov, V., Haim, D., Grossman, B., Mason, W.H., Watson, L.T., and Haftka, R.T., "Multidisciplinary Optimization of a Supersonic Transport Using Design of Experiments Theory and Response Surface Modeling," The Aeronautical Journal, pp. 347-356, October 1997.

[11]Hutchison, M.G., Unger, E.R., Mason, W.H., Grossman, B., Haftka, R.T., "Variable Complexity Aerodynamic Optimization of a High Speed Civil Transport Wing," Journal of Aircraft, Vol. 31, No. 1, pp. 110-116, 1994.

[12]McCullers, L.A., *FLOPS User's Guide, Release 5.81*, NASA Langley Research Center.

[13]Lamar, J.E., "A Vortex Lattice Method for the Mean Camber Shapes of Trimmed Non-Coplanar Planforms with Minimum Vortex Drag," NASA TN D-8090, June, 1976

[14]Gimmestad, D., "An Aeroelastic Optimization Procedure for Composite High Aspect Ratio Wings," AIAA Paper No. 79-0726, 20th Structures, Structural Dynamics, and Materials Conference, St. Louis, MO, April 4-6, 1979, pp. 79-86

[15]Gern, F.H., Sulaeman, E., Naghshineh-Pour, A., Kapania, R.K., and Haftka, R.T., "Flexible Wing Model for Structural Wing Sizing and Multidisciplinary Design Optimization of a Strut-Braced Wing," AIAA Paper 2000-1427, *41st AIAA/ASME/ASCE/AHS/ASC Structures, Structural Dynamics, and Materials Conference and Exhibit*, Atlanta, GA, April 3-6, 2000

[16]Torenbeek, E., "Development and Application of a Comprehensive, Design Sensitive Weight Prediction Method for Wing Structures of Transport Category Aircraft," Delft University of Technology, Report LR-693, Sept. 1992.

[17]Vanderplaats Research & Development, Inc., *DOT User's Manual*, Version 4.20, Colorado Springs, CO, 1995.

[18]Hoerner, S. F., Fluid-Dynamic Drag: Practical Information on Aerodynamic Drag and Hydrodynamic Resistance, pp. 8-1-8-20, published by S.F. Hoerner, Midland Park, N.J., 1965.

[19]Tetrault, P. A., Schetz, J. A., and Grossman, B., "Numerical Prediction of the Interference Drag of a Streamlined Strut Intersecting a Surface in Transonic Flow", AIAA Paper 2000-0509, 38th Aerospace Sciences Meeting and Exhibit, Reno, Nevada, 10-13 January, 2000.

[20]Tetrault, P. A., "Numerical Prediction of the Interference Drag of a Streamlined Strut Intersecting a Surface in Transonic Flow", Ph.D. dissertation, Virginia Polytechnic Institute & State University, 2000. (Available at http://etd.vt.edu).

[21]Gundlach, J.F., "Multidisciplinary Design Optimization and Industry Review of a 2010 Strut-Braced Wing Transonic Transport", MAD 99-06-03, 1999

[22]Braslow, A.L., Maddalon, D.V., Bartlett, D.W., Wagner, R.D., and Collier, F.S., "Applied Aspects of Laminar-Flow Technology," *Viscous Drag Reduction in Boundary Layers*, AIAA, Washington D.C., 1990, pp. 47-78

[23]Roskam, J., and Lan, C.-T. E., *Airplane Aerodynamics and Performance*, DARCorporation, Lawrence, KS, 1997

[24]Torenbeek, E., *Synthesis of Subsonic Airplane Design*, Delft University Press, Delft, The Netherlands, 1982

[25]Jensen, S.C., Rettie, I.H., and Barber, E.A., "Role of Figures of Merit in Design Optimization and Technology Assessment," Journal of Aircraft, Vol. 18, No. 2, February 1981, pp.76-81.

[26]Grasmeyer, J.M., "A Discrete Vortex Method for Calculating the Minimum Induced Drag and Optimum Load Distribution for Aircraft Configurations with Noncoplanar Surfaces." VPI-AOE-242, Department of Aerospace and Ocean Engineering, Virginia Polytechnic Institute and State University, Blacksburg, Virginia 24061, January 1998.

[27]Grasmeyer, J.M., "Stability and Control Derivative Estimation and Engine-Out Analysis.", VPI-AOE-254, Department of Aerospace and Ocean Engineering, Virginia Polytechnic and State University, Blacksburg, Virginia 24061, January 1998.